Article

Chemistry & Biology

Multimerization of a Proline-Rich Antimicrobial Peptide, Chex-Arg20, Alters Its Mechanism of Interaction with the *Escherichia coli* Membrane

Graphical Abstract

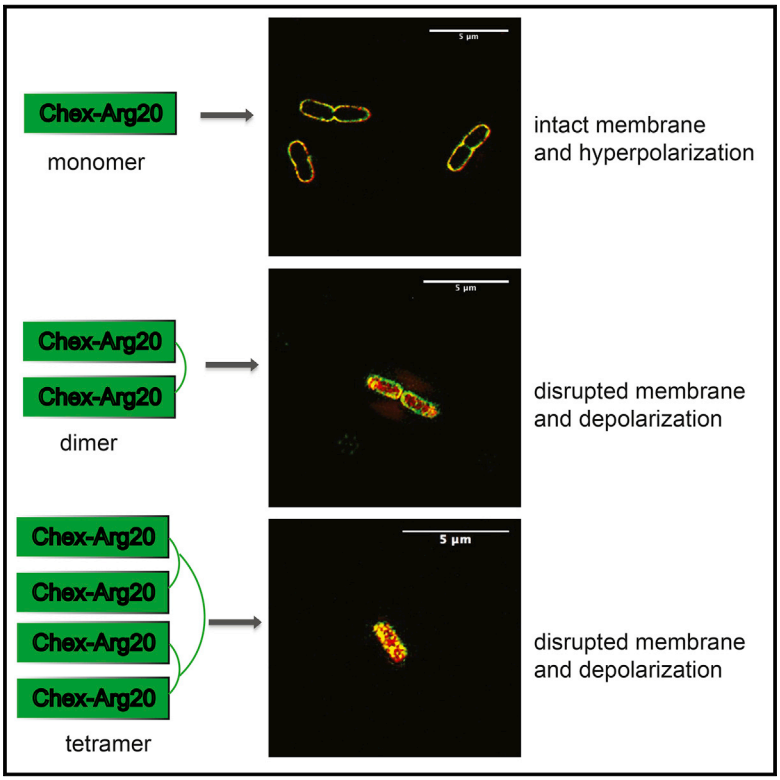

Authors

Wenyi Li, Neil M. O'Brien-Simpson, Julien Tailhades, ..., Frances Separovic, Mohammed Akhter Hossain, John D. Wade

Correspondence

john.wade@florey.edu.au (J.D.W.), akhter.hossain@florey.edu.au (M.A.H.)

In Brief

Li et al. show that *Escherichia coli* membrane interaction and permeability of a designed proline-rich antimicrobial peptide, Chex-Arg20, is significantly altered by its covalent multimerization. With an increase from monomer to tetramer, the mechanism proceeds from membrane aggregation and non-lysis to membrane damage.

Highlights

- Multimers of the proline-rich antimicrobial peptide, ChexArg20, were prepared
- Increase in peptide valency alters its *Escherichia coli* membrane interaction
- Change is from membrane non-lytic to membrane disruption
- There is also simultaneous change from membrane hyperpolarization to depolarization

Li et al., 2015, Chemistry & Biology *22*, 1250–1258
September 17, 2015
http://dx.doi.org/10.1016/j.chembiol.2015.08.011

CellPress

Chemistry & Biology
Article

Multimerization of a Proline-Rich Antimicrobial Peptide, Chex-Arg20, Alters Its Mechanism of Interaction with the *Escherichia coli* Membrane

Wenyi Li,[1,2] Neil M. O'Brien-Simpson,[3,4] Julien Tailhades,[2] Namfon Pantarat,[3] Raymond M. Dawson,[5] Laszlo Otvos, Jr.,[6,7] Eric C. Reynolds,[3,4] Frances Separovic,[1,4] Mohammed Akhter Hossain,[1,2,*] and John D. Wade[1,2,*]
[1]School of Chemistry, University of Melbourne, VIC 3010, Australia
[2]The Florey Institute of Neuroscience and Mental Health, University of Melbourne, VIC 3010, Australia
[3]Oral Health CRC, Melbourne Dental School, University of Melbourne, VIC 3010, Australia
[4]Bio21 Institute, University of Melbourne, VIC 3010, Australia
[5]Land Division, Defence Science and Technology Organization, Fishermans Bend, VIC 3207, Australia
[6]Department of Biology, Temple University, Philadelphia, PA 19122, USA
[7]Institute of Medical Microbiology, Semmelweis University, Budapest 1089, Hungary
*Correspondence: john.wade@florey.edu.au (J.D.W.), akhter.hossain@florey.edu.au (M.A.H.)
http://dx.doi.org/10.1016/j.chembiol.2015.08.011

SUMMARY

A3-APO, a de novo designed branched dimeric proline-rich antimicrobial peptide (PrAMP), is highly effective against a variety of in vivo bacterial infections. We undertook a selective examination of the mechanism for the Gram-negative *Escherichia coli* bacterial membrane interaction of the monomer (Chex-Arg20), dimer (A3-APO), and tetramer (A3-APO disulfide-linked dimer). All three synthetic peptides were effective at killing *E. coli*. However, the tetramer was 30-fold more membrane disruptive than the dimer while the monomer showed no membrane activity. Using flow cytometry and high-resolution fluorescent microscopy, it was observed that dimerization and tetramerization of the Chex-Arg20 monomer led to an alteration in the mechanism of action from non-lytic/membrane hyperpolarization to membrane disruption/depolarization. Our findings show that the membrane interaction and permeability of Chex-Arg20 was altered by multimerization.

INTRODUCTION

The widespread emergence of multidrug-resistant (MDR) bacterial infections has led to increased interest in the search for new antibiotics (Gammon, 2014). Antimicrobial peptides (AMPs) are considered as potential alternatives to conventional antibiotics, as they possess broad-spectrum activity and distinct modes of action that are based on their compositional and structural diversity (Jenssen et al., 2006). Most AMPs possess the ability to disrupt bacterial membranes through the formation of different pore structures as well as inhibiting intracellular targets, which can occur without causing membrane disruption (Brogden, 2005; Zasloff, 2002). Among the various types of AMPs, proline-rich AMPs (PrAMPs), which are typically found in insects and higher-order animals, show particular efficacy against systemic infections caused by Gram-negative bacteria. They display multimodal in vivo activity that include a combination of cell-penetrating capacity, targeting of several intracellular components including the 70-kDa bacterial heat shock protein DnaK causing interference with bacterial protein folding, and immunomodulatory activity (Li et al., 2014). Importantly, the PrAMPs, apidaecins, Bac7, and oncosins, were recently shown to bind with nanomolar dissociation constants to the 70S ribosome, leading to blockade of protein biosynthesis (Krizsan et al., 2014; Mardirossian et al., 2014). Tertiary structural analyses have since shown that oncosin acts by simultaneously obstructing the peptidyl transferase center and the peptide-exit tunnel of the ribosome (Roy et al., 2015; Seefeldt et al., 2015). PrAMPS also have very low toxicity toward host cells (Li et al., 2014). These features have highlighted the considerable potential of PrAMPs as replacements of, or supplements to, conventional antibiotics.

The peptide, Chex-Arg20, was de novo designed based on native PrAMPs with additional sequence optimization to enhance bacterial membrane penetration (Otvos et al., 2005; Rozgonyi et al., 2009). The branched dimeric form of A3-APO displays extensive and potent activity against Gram-negative bacteria including against MDR microbes in vitro, but also decreases the mortality and bacterial load in mouse models infected by MDR microbes in vivo (Ostorhazi et al., 2011a, 2011b; Otvos et al., 2014; Szabo et al., 2010). Furthermore, by inhibiting the folding of enzymes responsible for bacterial resistance, A3-APO in combination with conventional antibiotics either partially or fully restores their lost activities against MDR pathogens (Cassone and Otvos, 2010; Cassone et al., 2008; Otvos et al., 2006). The ability of A3-APO to inhibit protein refolding in bacteria also leads to decreased bacterial toxin production in vitro and increased survival time in animal models (Otvos et al., 2014).

A3-APO has been shown to degrade in vivo into several fragments, including the single-chain analog Chex-Arg20 peptide that exhibits equal or even better activity than its parental peptide, depending upon the selected cell line in vitro and the infection model in vivo (Li et al., 2015; Noto et al., 2008; Ostorhazi et al., 2013). To gain a better understanding of the mechanism

Table 1. Structure and Activity of PrAMP Analogs

PrAMP	Sequence	MIC (μM)	MBC (μM)	MPC (μM)[a]
Monomer	Chex-RPDKPRPYLPRPRPPRPVR —NH_2	28.6 ± 0.4	38.0 ± 0.9	>100
Dimer, A3-APO	Chex-RPDKPRPYLPRPRPPRPVR \ Dab—NH_2 / Chex-RPDKPRPYLPRPRPPRPVR	13.2 ± 1.7	23.9 ± 3.8	15.0 ± 0.2
Tetramer	(Chex-RPDKPRPYLPRPRPPRPVR \ Dab—C(S)—NH_2 / Chex-RPDKPRPYLPRPRPPRPVR)$_2$	22.6 ± 1.2	37.8 ± 0.1	0.5 ± 0.1

[a]For conversion of MIC/MBC and MPC values into mg/l, use a multiplication factor of 2.5 for the monomer, 5 for the dimer, and 10 for the tetramer.

of action, we undertook a detailed study using both flow cytometry and high-resolution microscopy of the effect on the *Escherichia coli* membrane of the Chex-Arg20 monomer, its dimer (A3-APO). For the purpose of comparison, a novel tetramer, i.e., a dimer of A3-APO connected by a disulfide bridge, was also examined. The results revealed important mechanistic differences between the three peptides, with important implications for the design of novel PrAMPs.

RESULTS AND DISCUSSION

Synthesis of Chex-Arg20 Multimer Analogs

The Chex-Arg20 monomer and its A3-APO dimer were synthesized by solid-phase peptide synthesis as previously described (Otvos et al., 2005). A similar synthesis approach involving an additional round of 3,3′-diaminobenzidine (DAB) branching was initially used for the synthesis of the tetramer. However, target peptide could not be obtained for each of the chemical strategies trialed, e.g., decreasing the resin loading, changing resin type, and replacing Lys with DAB. For this reason, a simple strategy of disulfide-mediated dimerization was used. A3-APO was thus assembled containing an additional cysteine at the C terminus (Figure S1; **1**). A portion was subjected to Cys thiol activation by 2,2′-dithiobis(5-nitropyridine) (DTNP) to yield **2** (Figure S1; **2**). The tetramer (dimerization of A3-APO) (Figure S1; **3**) was obtained by the combination of (**1**) and (**2**) in guanidine hydrochloride buffer (pH 8.5) in quantitative yield (Figure S1). All peptides were subjected to comprehensive chemical characterization by analytical reversed-phase high-performance liquid chromatography (RP-HPLC) and MALDI-TOF mass spectrometry to confirm their high purity (Figure S2).

Antibacterial Assay and *E. coli* Membrane Action

Each peptide (monomer, dimer, and tetramer) was tested for antibacterial activity against the Gram-negative bacterium *E. coli* in Luria-Bertani broth (LB). The minimum inhibitory concentration (MIC) and minimum bactericidal concentration (MBC) were determined, and microbial flow cytometry was used to monitor membrane integrity/permeability to the fluorescent dye propidium iodide (PI) (membrane permeabilizing concentration [MPC]) (López-Amorós et al., 1995) for each peptide (Figure S3). The MIC was determined by plotting maximal growth versus peptide concentration, according to the Lambert and Pearson analysis method, while MBC was confirmed via colony-forming unit (CFU) measuring assay (Lambert and Pearson, 2000; Sani et al., 2013). The MIC and MBC values for the monomer and dimer were similar to that induced by the tetramer (Table 1). However, to investigate the mode of antibacterial action, we used flow cytometry to measure the membrane integrity of *E. coli* incubated with the peptides, and found that the tetramer had a significantly ($p < 0.01$) lower MPC value than the monomer or dimer (Table 1). The MIC, MBC, and MPC values for A3-APO were found to be statistically equivalent but, conversely, the monomer failed to induce persistent membrane permeabilization. Figures 1A, 1B, 1C, and S3 show representative flow cytometry plots of *E. coli* incubated with each peptide at various concentrations, and clearly indicate that both A3-APO and the tetramer permeabilized the bacterial membrane whereas the monomer, even at the highest concentration tested, did not. The mechanism of action reported for the monomer is binding and inhibiting the function of a number of cytosolic bacterial proteins (Cassone et al., 2008). Thus, the lack of membrane permeabilization caused by the monomer is consistent with these findings. A3-APO has also been shown to bind and inhibit cytosolic protein folding and function (Zahn et al., 2013). However, our data also confirm that it has an additional mode of action, that of membrane permeabilization. The consistency between the MIC, MBC, and MPC values for A3-APO indicates that no one mechanism is dominant and that there is, probably, synergy between the modes of antibacterial actions. Interestingly, the flow cytometry data, but not the growth-based assays, clearly demonstrated that multimerization of the Chex-Arg20 monomer into A3-APO and the tetramer alters the mode of action from non-lytic to a membrane disruptive capacity.

Despite the very potent membrane permeabilizing activity of the tetramer, the MIC and MBC values were higher and equivalent to Chex-Arg20 monomer and A3-APO (dimer) (Table 1). Apart from valency, the sole difference between the tetramer and A3-APO is the disulfide bridge used to attach two A3-APO peptides together forming the tetramer. Antimicrobial peptides that are known to induce membrane disruption act on the inner/cytoplasmic membrane, which is known to contain disulfide

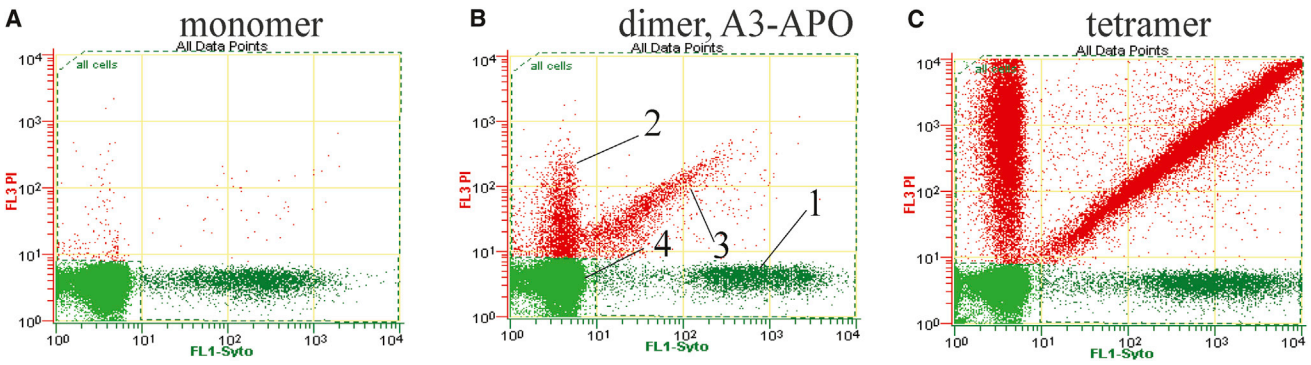

Figure 1. Graphical Representation of the Determination of the MPC

(A) Monomer, (B) A3-APO, and (C) tetramer against *E. coli* preincubated at 37°C, in which viable whole cells (region 1, SYTO9+ cells), dead whole cells (region 2, 3, PI+ cells), and cell debris (region 4, SYTO9− and PI−). See also Figure S3.

bond-reducing proteins and have a redox potential that favors disulfide bond disruption (Eser et al., 2009; Kadokura et al., 2003). Furthermore, the bacterial membrane is highly fluid and dynamic, and the lytic action of some AMPs has been shown to be reversible (Gee et al., 2013; Hall et al., 2014; Lee et al., 2014). Thus the decline in activity from that measured by flow cytometry (MPC) and that measured by the growth assays (MIC and MBC) is probably due to two factors: the fluid/dynamic nature and disulfide bond-reducing environment of the inner membrane. To assess this possibility, the MPC against *E. coli* of the membrane-active tetramer was evaluated at different times of incubation, and compared with control AMPs. The time course showed that the concentration of tetramer needed to disrupt the bacterial membrane increased as a function of incubation time, which suggests that reduction of the disulfide bond occurred on culture with *E. coli* (Figure 2A). As further evidence, samples of the tetramer and bacteria co-cultured after 14 hr were lysed via sonication, and both tetramer and degraded products were isolated and analyzed by RP-HPLC. The two principal peaks were identified as corresponding to tetramer and A3-APO-Cys (Figure 2B).

These results show that the tetramer rapidly permeabilizes the membranes of Gram-negative bacteria at a significantly lower concentration than the A3-APO (dimer). However, the inner membrane environment leads to disulfide bond reduction of the tetramer to its A3-APO (dimer) components and an apparent decrease in antimicrobial activity (MIC, MBC), albeit to the same level as the dimer. Given that tetramer reduction is only about 50% complete after 14 hr, it is to be expected that the assay results will reflect a mixture of degradation outcomes. Furthermore, the breakdown of the tetramer itself is not simple and does not lead to two identical A3-APO molecules, but rather to modified A3-APO that contain a terminal Cys residue. This will mean they will not have the same AMP activity as shown in the previous study (Li et al., 2015). Therefore, the observed decrease in activity of the reduced tetramer is a partial reflection of the reduced/modified version simply not behaving as an A3-APO molecule. Given the complex interactions shown by A3-APO in killing bacteria, this would have an impact on activity. Work is under way on the preparation of a non-reducible tetramer. These results similarly indicate that the bacterial membrane is not a static environment, and the capacity of the disulfide bond to be reduced within the inner membrane interface of bacteria, as well as being an important factor in AMP design, also suggests a useful strategy for delivery of drugs via antimicrobial peptides. Reversible disulfide linkages have been extensively utilized in drug discovery to release final drug compositions from prodrugs (Saito et al., 2003).

Peptide Localization in *E. coli*

Given that the mechanism of membrane action of Chex-Arg20 varies with the extent of multimerization, we used both flow cytometry and high-resolution microscopy to determine whether the interaction of peptide and bacteria correlates with membrane lysis and to determine where the peptides localize in the bacteria. Fluorescent analogs of the peptides were prepared via the metal-free thiol-maleimide coupling reaction (Nguyen et al., 2013; Pounder et al., 2008). A fluorescein label, fluorescein isothiocyanate (FITC), was judiciously placed at the C terminus of each peptide, which were then co-cultured with *E. coli* and analyzed by flow cytometry with additional PI fluorescence to indicate membrane disruption (Figure S4). The uptake of FITC-peptide and PI was calculated by the ratio of the green fluorescein fluorescence or the red PI fluorescence to total fluorescence population (Figure 3). The addition of the fluorophore did not lead to significant inactivation of the peptides (Table S1). With increasing peptide concentration, there was a corresponding increase in FITC-monomer associated with *E. coli* cells, with 100% FITC-monomer-positive bacteria correlating with the MIC and MBC (Figure 3, see also Table S1). Consistent with the monomer MPC data, there was no uptake of the membrane-permeable indicator dye, PI, with increasing monomer concentration. FITC-A3-APO and FITC-tetramer showed a similar trend of bacterial uptake of peptide compared with the labeled monomer. However, for both peptides there was a corresponding increase in PI-positive bacteria, which is consistent with the ability of A3-APO and the tetramer to induce membrane lysis (Figure 3). Hence, as determined by PI inclusion, the membrane lytic mechanism of A3-APO and the tetramer correlates with peptide association for bacteria and is related to the concentration dependence for the mechanism alteration (Hernandez-Gordillo et al., 2014; Paulsen et al., 2013; Podda et al., 2006; Végh et al.,

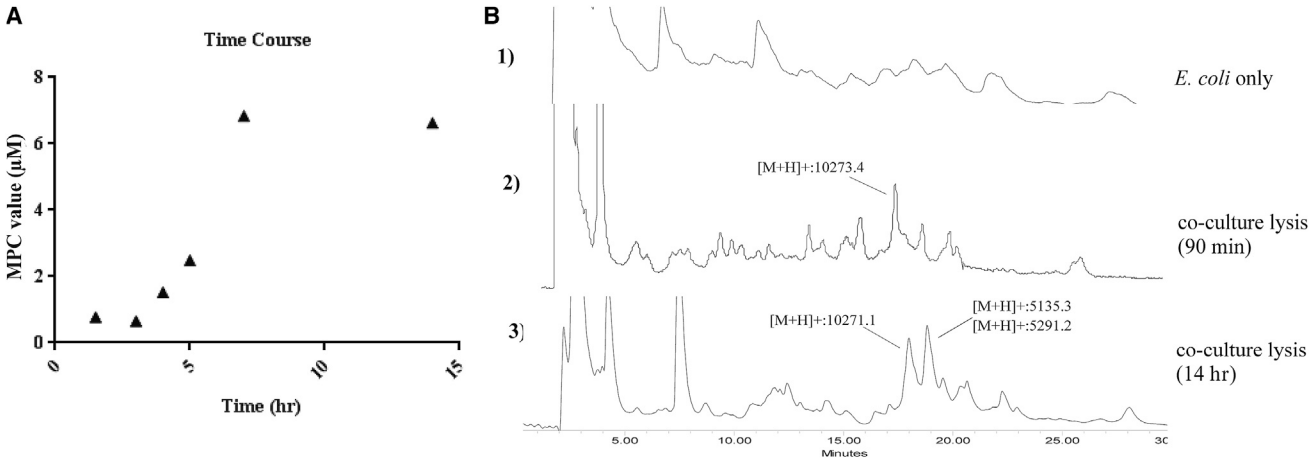

Figure 2. Stability of Tetramer in *E. coli* Culture

(A) MPC time course of tetramer. Data are expressed as the concentration of peptide (μM) that causes 100% of bacterial cells to have a permeabilized membrane (triangles).

(B) RP-HPLC of the tetramer co-cultured with *E. coli*. Lysate of: (1) *E. coli* only, (2) *E. coli* incubated with the tetramer after 90 min, and (3) after 14 hr incubation. Calculated [M + H]: tetramer = 10,270.5; A3-APO-Cys-NH_2 = 5136.1.

2011). A trend analysis on the FITC-peptide-positive bacteria and PI-positive bacteria found that there was a significant ($p < 0.01$) positive correlation between membrane disruption and peptide-bound bacteria for A3-APO ($R^2 = 0.98$) and tetramer ($R^2 = 0.97$) but not for the monomer ($R^2 = 0.27$).

The flow cytometry data showed that the monomer, dimer, and tetramer each associate with the bacteria, but did not show where each peptide localized with increasing concentration. To investigate this aspect, Alexa Fluor 647-labeled peptides were assembled using the same chemistry as described above. Alexa Fluor dyes are superior to FITC in that they have longer photo-bleaching half-life and are thus suitable for high-resolution microscopy. Addition of the Alexa Fluor label to the peptides had the same effect as FITC on peptide antimicrobial activity (Table S1). For image analysis, *E. coli* membranes were labeled with FM lipophilic styryl dye (FM 4-64FX, green fluorescence) and incubated (same times as above) with the Alexa Fluor 647-labeled peptides (red fluorescence), and the peptide-bacteria interaction then was visualized using an Applied Precision Deltavision OMX V4 Blaze structured illumination microscope (Figure 4; a yellow/orange fluorescence indicates co-localization of peptide and membrane). With increasing concentrations (6–24 μM), the Alexa Fluor 647-monomer initially localized to the membrane of the bacteria, and as the peptide concentration increased the fluorescence of the membrane increased (Figure S5). Although the monomer is evidently localized at the membrane at all concentrations tested, it is also apparent that it is within the cytoplasm, appearing as discrete foci (red spots). At a concentration of 6 μM, the peptide can also be seen to be only within the cytoplasm, as indicated by the bacteria with a green fluorescent membrane and red fluorescent spots within the bacteria (Figure S5). These results are consistent with previous reports that the monomer is known to bind to cytoplasmic proteins and inhibit their function, resulting in the death of the bacteria (Zahn et al., 2013). Compared with the monomer, both labeled A3-APO and tetramer initially interact with the bacterial membrane at the lowest concentration (6 μM), causing membrane disruption, as evident from the ruffling and broken staining of the bacteria (Figures S5B and S5C). As peptide concentration increased, both A3-APO and tetramer localized primarily in the cytosol, then, at higher concentrations, the peptides associated with both the cytosol and membrane. Interestingly, both A3-APO and the tetramer have a similar pattern of localization compared with the known cell-penetrating peptide Arginine-9 (Figure S5D). Our data clearly show that the Chex-Arg20 monomer, A3-APO, and tetramer all interact with the membrane of the bacteria, and that they localize to the cytosol of the bacteria as the peptide concentration increases. It is clear that membrane interaction of A3-APO and the tetramer induce membrane lysis, whereas the monomer does not. However, the monomer clearly interacts with the bacterial membrane; to investigate whether the monomer affects the bacterial membrane, the membrane potential of the bacteria incubated with each of the peptides was analyzed.

Analysis of Membrane Potential

A number of non-lytic traditional antibiotics, such as gramicidin and valinomycin, act as ionophores, allowing diffusion of specific ions across the membrane and down concentration gradients by forming ion channels (Harold and Baarda, 1967; Separovic et al., 1994). This facilitated diffusion of ions results in alteration of the membrane potential, causing depolarization of the membrane, which is typical of gramicidin and pore-forming or lytic AMPs (Wu et al., 1999), whereas valinomycin, although acting as a K^+-specific ionophore, induces a hyperpolarized membrane state in low K^+ environments. Some highly cationic AMPs have been reported to produce a hyperpolarized membrane by lying on top of the lipid membrane (Hong and Su, 2011).

The membrane potential of *E. coli* with the peptides was measured using the Invitrogen BacLight bacterial membrane potential kit to determine the capacity of the peptides to alter

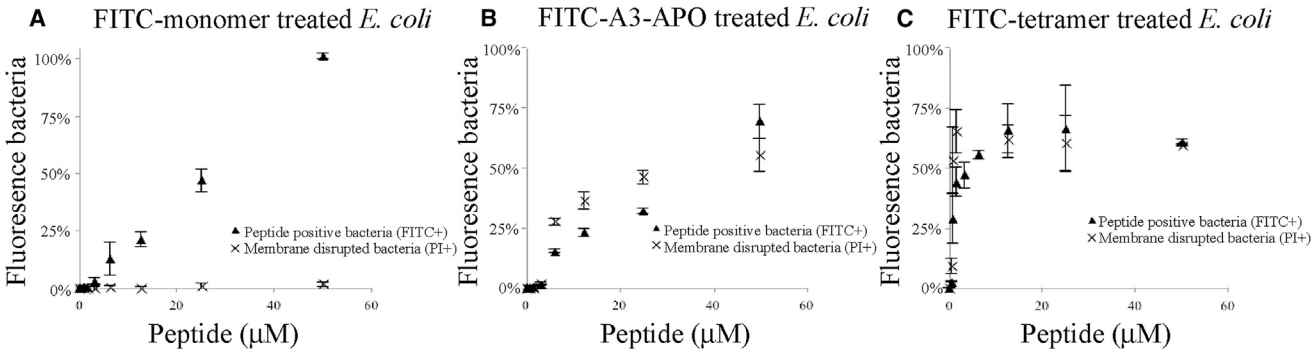

Figure 3. Percentage Uptake of Fluorescein-Labeled Peptides

(A) FITC-monomer-treated *E. coli*, (B) FITC-A3-APO-treated *E. coli*, (C) FITC-tetramer-treated *E. coli*. The percentage of peptide-positive bacteria (FITC+) and membrane-disrupted bacteria (PI+) were determined by flow cytometry. Crosses indicate membrane-disrupted bacteria (PI+); triangles indicate peptide-positive bacteria (FITC+). All data are expressed as mean ± standard deviation as indicated by the error bars, based on values obtained from at least two biological replicates. See also Figure S4.

membrane potential. Bacteria were incubated with each peptide at half, equal, and double the MIC, stained with the membrane potential (ion sensitive/response) fluorophore 3,3′-diethyloxacarbocyanine iodide ($DiOC_2$), and membrane potential was determined by flow cytometry (Figure S6). The *E. coli* normal membrane potential state (−CCCP) and fully depolarized state after incubation with carbonyl cyanide 3-chlorophenylhydrazone (+CCCP) are shown in Figures S6A and S6B, respectively. From the flow cytometry dot plots, each peptide can be seen to have distinct actions on *E. coli* membranes. The increase in red fluorescence in the bacterial population incubated with the monomer compared with the normal/untreated cells is indicative of a hyperpolarized membrane. A3-APO increased the red fluorescence also but induced a shift in the green fluorescent population as peptide concentration increased, indicating a shift from a mixed hyperpolarized and depolarized cell population to a more depolarized membrane population. The effect of the tetramer on *E. coli* was to induce a depolarized cell population. Figure 5 shows the calculated membrane potential and clearly demonstrates that the monomer led to a strongly hyperpolarized state, and A3-APO to a depolarized state, while the tetramer induced a strongly depolarized population. The ability of the monomer to induce a hyperpolarized membrane indicates that these peptides clearly have more than one mode of antimicrobial action, which is consistent with previous reports that both the monomer and A3-APO also bind to cytosolic proteins and induce cell death via this mechanism (Cassone et al., 2008), but here it is shown that both these peptides alter the membrane potential with the monomer having a potential ionophore mechanism, whereas both A3-APO and the tetramer have a membrane-depolarizing/lytic function. The ability of the monomer to hyperpolarize bacterial membranes may increase susceptibility to host antimicrobial peptides. Indeed, Gries et al. have shown that bacteria with hyperpolarized membranes are more susceptible to cationic antimicrobial peptides (Gries et al., 2013). This mechanism may in part explain the finding that the monomer and A3-APO are more effective in vivo (Ostorhazi et al., 2011a, 2011b; Otvos et al., 2014; Szabo et al., 2010), as a bacterial infection would induce the release of AMPs from host cells such as neutrophils.

General Discussion

There remains no universal agreement within the AMP research community as to the precise mechanism of AMP membrane interaction and corresponding antibacterial activity. However, Vivcharuk and Kaznessis (2010) showed that an AMP dimer has greater peptide-membrane attraction than the monomer counterpart. Therefore, we believe a plausible explanation for our findings is that a dimer/tetramer has a wider, highly positively charged ''carpet-like'' surface leading to increased binding. This is supported by our results showing clearly that the monomer does interact with the membrane (high-resolution microscopy imaging and membrane potential assay); moreover, as valency is increased there is a corresponding increase in the attraction of the multimer to the membrane and, hence, a change in mechanism from non-disruptive to disruptive.

Finally, there are few other examples of the effects of dimerization or multimerization on other PrAMPs. It previously shown that the PrAMP, pyrrhocoricin, was more active as a dimer, an effect attributed to better efficacy on bacterial membranes (Cudic et al., 2002). This formed the basis of our many studies on A3-APO and its analogs. Furthermore, Dempsey et al. (2003 and Zhou et al. (2011) showed that a dimer of a peptide monomer becomes more membrane disruptive. Hernandez-Gordillo et al. (2014) also showed that a dimer of another designed PrAMP possessed increased antibacterial potency. At MIC, it showed no bacterial membrane disruption but did cause rupture at higher concentrations. It remains to be determined whether this can be shown for PrAMPs in general, but we anticipate that our results will provide significant motivation for others to examine this possibility.

In summary, multimerization of the designed PrAMP, Chex-Arg20, leads to an alteration in the mechanism of interaction with the membrane of the Gram-negative bacterium *E. coli*. With an increase from monomer to tetramer, the mechanism proceeds from membrane aggregation and non-lysis to membrane damage, as indicated by MPC via flow cytometry and image analysis by high-resolution microscopy. Meanwhile, the membrane potential assay showed that the monomer hyperpolarized the bacterial membrane while the dimer caused membrane polarization that changed to depolarization as concentration increased. Furthermore, the tetramer displayed a much more

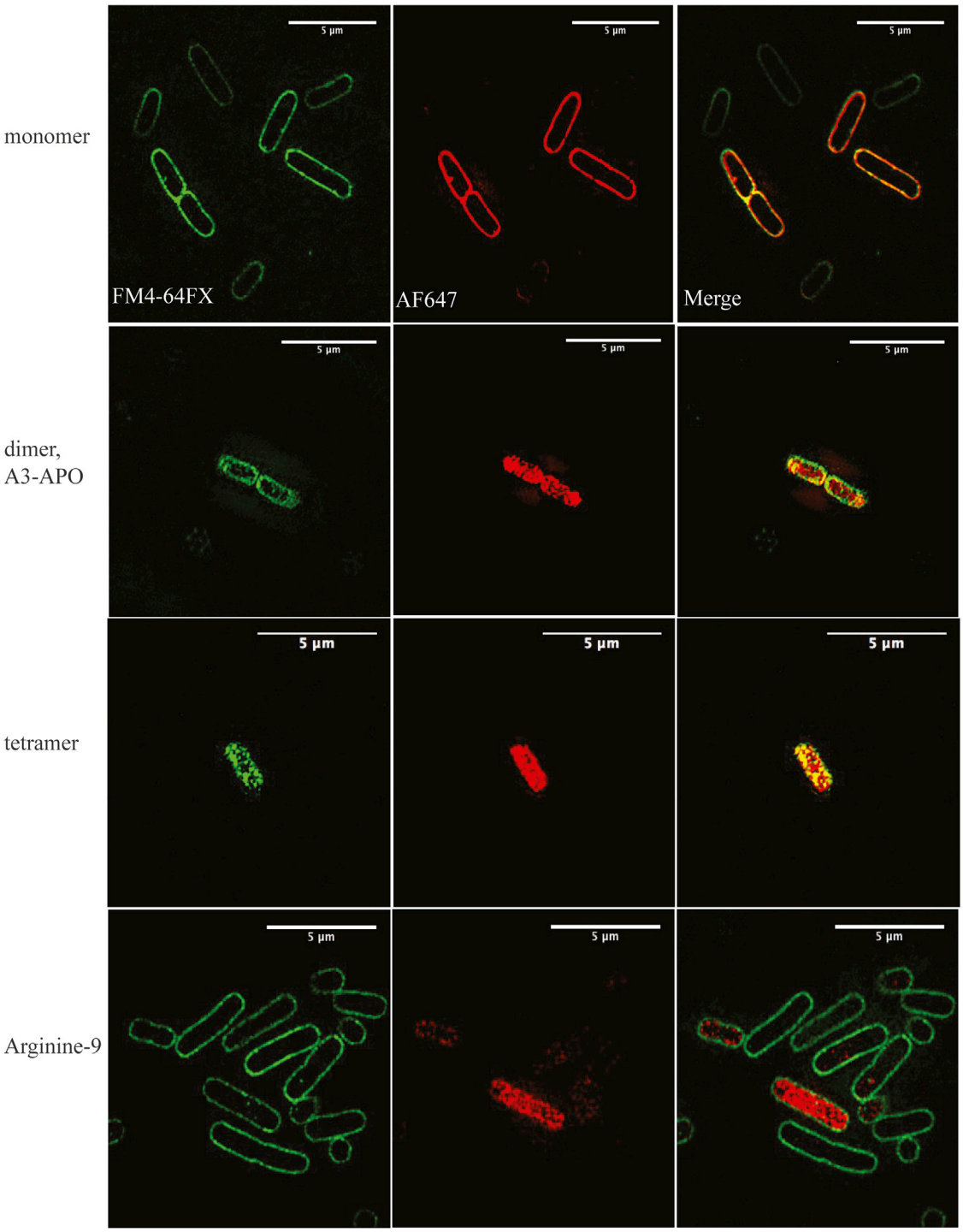

Figure 4. Representative Image Analysis of Alexa Fluor 647-Labeled Peptide at 12 μM, Co-cultured with *E. coli*

Applied Precision Deltavision OMX V4 Blaze Structured Illumination Microscope used with membrane stain FM4-64FX dye (green) and Alexa Fluor 647 (red) labeled monomer, A3-APO, tetramer, and Arginine-9 treated samples. Lipid membranes are shown as green fluorescence; red fluorescence indicates Alexa Fluor 647-labeled peptide; yellow/orange fluorescence indicates co-localization of lipid membrane and peptide. See also Figure S5.

potent ability to depolarize membranes, even at low concentration. Importantly, none of the peptides display hemolytic activity or cytotoxicity (Table S2). These findings aid the understanding of the action of PrAMPs with multiple mechanisms of action as well as novel cell-penetrating peptides. For example, the increased membrane rupture by dimers and tetramers suggests that covalent combination with conventional antibiotics may enable a more effective means of bacterial killing, which might

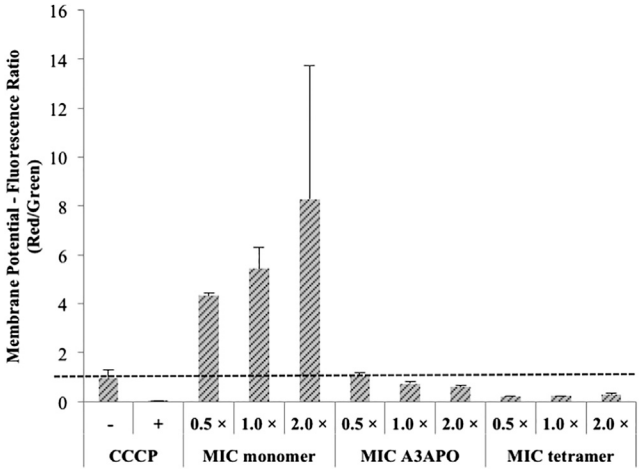

Figure 5. Detection of Membrane Potential in *E. coli* with Serial Peptide Addition

Red/green ratios were calculated using mean fluorescence intensities of populations incubated with 30 μM $DiOC_2$ for 30 min in the presence or absence of CCCP and with 0.5× MIC, 1× MIC, and 2× MIC of monomer, A3-APO, or tetramer. All data are expressed as mean ± standard deviation as indicated by the error bars, based on values obtained from at least two biological replicates. See also Figure S6.

not otherwise be possible with the monomer. Furthermore, a dimer of two different PrAMPs may afford greater bacterial killing selectivity or intracellular targeting.

SIGNIFICANCE

The widespread emergence of antibiotic resistance and the paucity of novel and effective treatments have stimulated much interest in antimicrobial peptides as potential therapeutics. In particular, PrAMPs, which are widely distributed in Nature, have a distinct portfolio of activity ranging from membrane rupture to blockade of ribosomal protein expression. This work sought to understand the mode of interaction with Gram-negative *E. coli* membrane interaction of the de novo designed PrAMP, Chex1-Arg20, and its discontinuous dimer, A3-APO, and of their permeability. For comparison, a disulfide dimer of A3-APO was also examined. The data showed that an increase in valency led to an alteration in the mechanism of action from non-lytic/membrane hyperpolarization to membrane disruption/depolarization. Furthermore, the *E. coli* membrane potential displayed differences between Chex1-Arg20 and multimers. This change in capacity was not correlated by proportional bacterial killing, highlighting the essential roles of other intracellular or immunological mechanisms in this process. Nevertheless, the distinctive, altered properties of these multimers advance our understanding of this type of AMP and suggest significant potential for the development of novel PrAMPs.

EXPERIMENTAL PROCEDURES

Materials

9-Fluoroenylmethoxylcarbonyl (Fmoc)-L-amino acids and *N*,*N*,*N*′,*N*′-tetramethyl-O-(1H-benzotriazol-1-yl)uranium-hexafluorophosphate (HBTU) were purchased from GL Biochem. TentaGel-MB-RAM-resin and TentaGel-R-RAM-resin were from Rapp Polymere. N,N-Diisopropylethylamine (DIPEA), dimethylformamide, and trifluoroacetic acid (TFA) were obtained from Auspep. Piperidine, triisopropylsilane (TIPS), anisole, 3,6-dioxa-1,8-octanedithiol (DODT), DTNP, and acetonitrile were all obtained from Sigma. Fluorescein-5-maleimide, FM4-64FX dye, Alexa Fluor 647-maleimide, SYTO9, and PI were purchased from Life Technology.

Solid-Phase Peptide Synthesis

The peptides (Table 1) were synthesized by Fmoc solid-phase methods (Fields and Noble, 1990). Peptide-chain assembly was carried out on a CEM Liberty (DKSH) microwave-assisted synthesizer or a Protein Technologies Tribute batch-wise peptide synthesizer using Fmoc Rink amide polystyrene resin. Standard Fmoc chemistry was used throughout with a 4-fold molar excess of the Fmoc-protected amino acids in the presence of 4-fold HBTU and 8-fold DIPEA. Non-natural amino acids were coupled manually to ensure completion of coupling reaction. The peptides were cleaved from the solid-support polystyrene resin with TFA in the presence of anisole, TIPS, and water as scavengers (ratio 95:3:1:1) for 2 hr at room temperature. After cleavage the resin was removed by filtration, the filtrate was concentrated under a stream of nitrogen, and the peptide products were precipitated in ice-cold diethyl ether, washed, and centrifuged three times. The peptides were then purified by RP-HPLC in water and acetonitrile with 0.1% TFA. The final products were monitored and characterized by RP-HPLC and MALDI-TOF mass spectroscopy. The tetramer was obtained by disulfide bond linkage between two molecules of A3-APO (see Supplemental Experimental Procedures). Peptide labeling with fluorescein-5-maleimide or Alexa Fluor 647-maleimide was achieved in the presence of peptide with PBS at pH 7.4 (see Supplemental Experimental Procedures).

Peptide Localization with *E. coli* ATCC 25922

Before the test, for the normal peptide, both SYTO9 and PI were added. By contrast, only PI was added to the fluorescein-labeled peptide samples. A3-APO and fluorescein-labeled monomer/A3-APO in LB (100 μl, from initial stock suspensions of 100 μM), 2 × 10^5 viable bacterial cells (100 μl of stock suspension, 2 × 10^5 CFU) were added and the mixtures, in 96-well flat-bottomed microtiter plates (Interpath Service) were incubated at 37°C for 90 min. The contents of the 96-well plates were monitored by Quanta flow cytometry.

Image Analysis

E. coli was grown in LB. Viable cells were diluted to 2.5 × 10^5 cells/ml in LB at 37°C immediately prior to incubation with Alexa Fluor 647-labeled peptides for 90 min. The co-culture samples were combined with labeled peptides at 6, 12, or 24 μM. The samples were then transferred to Eppendorf tubes, followed by washing with Hank's balanced salt solution (HBSS; Invitrogen) three times (5000 × *g*, 10 min at 4°C). The membrane stain FM4-64FX dye (Invitrogen) (5 μg/ml, 10 min, ice bath) was added to the above samples to bind the outer leaf of *E. coli* plasma membrane, followed by washing with HBSS three times (5000 × *g*, 10 min at 4°C). Finally, the samples were transferred to chambers coated with poly-D-lysine followed by fixation with 4% paraformaldehyde. After sample preparation, the samples were analyzed by an Applied Precision Deltavision OMX V4 Blaze structured illumination microscope (microscope lasers for FM4-64FX [568 nm] and Alexa Fluor 647 [642 nm] and filters: 609/37 for FM4-64FX and 683/40 for Alexa Fluor 647) (Figure S5). SoftWorx software was used for reconstruction and the Deltavision OMX Master Control Software was used for controls. Immersion oil with a refractive index of 1.514 was used for the microscope.

Membrane Potential Assay

Membrane potential was determined by flow cytometry using a BacLight Bacterial Membrane Potential Kit (Invitrogen). *E. coli* was inoculated to late exponential phase. Viable cells were then diluted to 2 × 10^6 cells/ml in PBS and incubated at 37°C with variable concentrations (0.5× MIC, 1× MIC, 2× MIC) of the tested peptides. The protonophore CCCP was added with final concentration 5 μM to the non-treated cells to provide a depolarized control, and 30 μM $DiOC_2$ was added to the rest of the samples. Membrane potential was determined by a flow cytometer as a ratio of the fluorescent cells between the red and green fluorescence. Gates were drawn based on the controls present in hyperpolarized, polarized, or depolarized regions.

After analysis and collection of the data, the membrane potentials were determined and normalized by the ratio of the population of red fluorescence (FL3) to green fluorescence (FL1) intensity (Figure S6).

SUPPLEMENTAL INFORMATION

Supplemental Information includes Supplemental Experimental Procedures, six figures, and two tables and can be found with this article online at http://dx.doi.org/10.1016/j.chembiol.2015.08.011.

AUTHOR CONTRIBUTIONS

W.L. performed most of the chemical syntheses and antibacterial experiments, and partially wrote the initial draft of the manuscript; N.P. helped with the antibacterial testing; J.T., L.O., M.A.H., and J.D.W. assisted with the design of the synthetic peptides; L.O., R.M.D., E.C.R., and F.S. analyzed the results; N.M.O'B.S., L.O., E.C.R., F.S., M.A.H., and J.D.W. co-supervised the study, analyzed the data, and co-wrote the manuscript.

ACKNOWLEDGMENTS

Super-resolution imaging was performed at the Materials Characterization and Fabrication Platform (MCFP) at the University of Melbourne. We thank Shu Lam and Greg Qiao (Chemical and Biomolecular Engineering, University of Melbourne) for assistance with application of their high-resolution fluorescent microscopy technique to our studies. We gratefully acknowledge support of the studies undertaken in the authors' laboratory by an ARC Discovery Project grant (DP150103522) to J.D.W. and M.A.H., and NHMRC Project grants (APP1029878) to N.M.O'B.S. and (APP1008106) to E.C.R. and N.M.O'B.S. J.D.W. is an NHMRC (Australia) Principal Research Fellow. W.L. is the recipient of an MIRS PhD award. Research at the FNI was also supported by the Victorian Government's Operational Infrastructure Support Program.

Received: June 11, 2015
Revised: July 28, 2015
Accepted: August 7, 2015
Published: September 17, 2015

REFERENCES

Brogden, K.A. (2005). Antimicrobial peptides: pore formers or metabolic inhibitors in bacteria? Nat. Rev. Microbiol. *3*, 238–250.

Cassone, M., and Otvos, L. (2010). Synergy among antibacterial peptides and between peptides and small-molecule antibiotics. Expert Rev. Anti Infect. Ther. *8*, 703–716.

Cassone, M., Vogiatzi, P., La Montagna, R., De Olivier Inacio, V., Cudic, P., Wade, J.D., and Otvos, L., Jr. (2008). Scope and limitations of the designer proline-rich antibacterial peptide dimer, A3-APO, alone or in synergy with conventional antibiotics. Peptides *29*, 1878–1886.

Cudic, M., Condie, B.A., Weiner, D.J., Lysenko, E.S., Xiang, Z.Q., Insug, O., Bulet, P., and Otvos, L., Jr. (2002). Development of novel antibacterial peptides that kill resistant isolates. Peptides *23*, 2071–2083.

Dempsey, C.E., Ueno, S., and Avison, M.B. (2003). Enhanced membrane permeabilization and antibacterial activity of a disulfide-dimerized magainin analogue. Biochemistry *42*, 402–409.

Eser, M., Masip, L., Kadokura, H., Georgiou, G., and Beckwith, J. (2009). Disulfide bond formation by exported glutaredoxin indicates glutathione's presence in the *E. coli* periplasm. Proc. Natl. Acad. Sci. USA *106*, 1572–1577.

Fields, G.B., and Noble, R.L. (1990). Solid phase peptide synthesis utilizing 9-fluorenylmethoxycarbonyl amino acids. Int. J. Pept. Protein Res. *35*, 161–214.

Gammon, K. (2014). Drug discovery: leaving no stone unturned. Nature *509*, S10–S12.

Gee, M.L., Burton, M., Grevis-James, A., Hossain, M.A., McArthur, S., Palombo, E.A., Wade, J.D., and Clayton, A.H.A. (2013). Imaging the action of antimicrobial peptides on living bacterial cells. Sci. Rep. *3*, 1557.

Gries, C.M., Bose, J.L., Nuxoll, A.S., Fey, P.D., and Bayles, K.W. (2013). The Ktr potassium transport system in *Staphylococcus aureus* and its role in cell physiology, antimicrobial resistance and pathogenesis. Mol. Microbiol. *89*, 760–773.

Hall, K., Lee, T.-H., Mechler, A.I., Swann, M.J., and Aguilar, M.-I. (2014). Real-time measurement of membrane conformational states induced by antimicrobial peptides: balance between recovery and lysis. Sci. Rep. *4*, 1–9.

Harold, F.M., and Baarda, J.R. (1967). Gramicidin, valinomycin, and cation permeability of *Streptococcus faecalis*. J. Bacteriol. *94*, 53–60.

Hernandez-Gordillo, V., Geisler, I., and Chmielewski, J. (2014). Dimeric unnatural polyproline-rich peptides with enhanced antibacterial activity. Bioorg. Med. Chem. Lett. *24*, 556–559.

Hong, M., and Su, Y. (2011). Structure and dynamics of cationic membrane peptides and proteins: insights from solid-state NMR. Protein Sci. *20*, 641–655.

Jenssen, H., Hamill, P., and Hancock, R.E.W. (2006). Peptide antimicrobial agents. Clin. Microbiol. Rev. *19*, 491–511.

Kadokura, H., Katzen, F., and Beckwith, J. (2003). Protein disulfide bond formation in prokaryotes. Annu. Rev. Biochem. *72*, 111–135.

Krizsan, A., Volke, D., Weinert, S., Strater, N., Knappe, D., and Hoffmann, R. (2014). Insect-derived proline-rich antimicrobial peptides kill bacteria by inhibiting bacterial protein translation at the 70S ribosome. Angew. Chem. Int. Ed. Engl. *53*, 12236–12239.

Lambert, R.J.W., and Pearson, J. (2000). Susceptibility testing: accurate and reproducible minimum inhibitory concentration (MIC) and non-inhibitory concentration (NIC) values. J. Appl. Microbiol. *88*, 784–790.

Lee, T.-H., Heng, C., Separovic, F., and Aguilar, M.-I. (2014). Comparison of reversible membrane destabilisation induced by antimicrobial peptides derived from Australian frogs. Biochim. Biophys. Acta *1838*, 2205–2215.

Li, W., Tailhades, J., O'Brien-Simpson, N., Separovic, F., Otvos, L., Jr., Hossain, M.A., and Wade, J. (2014). Proline-rich antimicrobial peptides: potential therapeutics against antibiotic-resistant bacteria. Amino Acids *46*, 2287–2294.

Li, W., Tailhades, J., Hossain, M.A., O'Brien-Simpson, N.M., Reynolds, E.C., Otvos, L., Separovic, F., and Wade, J.D. (2015). C-terminal modifications broaden activity of the proline-rich antimicrobial peptide, Chex1-Arg20. Aust. J. Chem. *68*, 1373–1378.

López-Amorós, R., Comas, J., and Vives-Rego, J. (1995). Flow cytometric assessment of *Escherichia coli* and *Salmonella typhimurium* starvation-survival in seawater using rhodamine 123, propidium iodide, and oxonol. Appl. Environ. Microbiol. *61*, 2521–2526.

Mardirossian, M., Grzela, R., Giglione, C., Meinnel, T., Gennaro, R., Mergaert, P., and Scocchi, M. (2014). The host antimicrobial Peptide bac71-35 binds to bacterial ribosomal proteins and inhibits protein synthesis. Chem. Biol. *21*, 1639–1647.

Nguyen, L.-T.T., Gokmen, M.T., and Du Prez, F.E. (2013). Kinetic comparison of 13 homogeneous thiol-X reactions. Polym. Chem. *4*, 5527–5536.

Noto, P.B., Abbadessa, G., Cassone, M., Mateo, G.D., Agelan, A., Wade, J.D., Szabo, D., Kocsis, B., Nagy, K., Rozgonyi, F., et al. (2008). Alternative stabilities of a proline-rich antibacterial peptide in vitro and in vivo. Protein Sci. *17*, 1249–1255.

Ostorhazi, E., Holub, M.C., Rozgonyi, F., Harmos, F., Cassone, M., Wade, J.D., and Otvos, L., Jr. (2011a). Broad-spectrum antimicrobial efficacy of peptide A3-APO in mouse models of multidrug-resistant wound and lung infections cannot be explained by in vitro activity against the pathogens involved. Int. J. Antimicrob. Agents *37*, 480–484.

Ostorhazi, E., Rozgonyi, F., Szabo, D., Binas, A., Cassone, M., Wade, J.D., Nolte, O., Bethel, C.R., Bonomo, R.A., and Otvos, L., Jr. (2011b). Intramuscularly administered peptide A3-APO is effective against carbapenem-resistant *Acinetobacter baumannii* in mouse models of systemic infections. Biopolymers *96*, 126–129.

Ostorhazi, E., Voros, E., Nemes-Nikodem, E., Pinter, D., Sillo, P., Mayer, B., Wade, J.D., and Otvos, L., Jr. (2013). Rapid systemic and local treatments with the antibacterial peptide dimer A3-APO and its monomeric metabolite

eliminate bacteria and reduce inflammation in intradermal lesions infected with *Propionibacterium acnes* and methicillin-resistant *Staphylococcus aureus*. Int. J. Antimicrob. Agents *42*, 537–543.

Otvos, L., Jr., Wade, J.D., Lin, F., Condie, B.A., Hanrieder, J., and Hoffmann, R. (2005). Designer antibacterial peptides kill fluoroquinolone-resistant clinical isolates. J. Med. Chem. *48*, 5349–5359.

Otvos, L., Jr., de Olivier Inacio, V., Wade, J.D., and Cudic, P. (2006). Prior antibacterial peptide-mediated inhibition of protein folding in bacteria mutes resistance enzymes. Antimicrob. Agents Chemother. *50*, 3146–3149.

Otvos, L., Flick-Smith, H., Fox, M., Ostorhazi, E., Dawson, R.M., and Wade, J.D. (2014). The designer proline-rich antibacterial peptide A3-APO prevents *Bacillus anthracis* mortality by deactivating bacterial toxins. Protein Pept. Lett. *21*, 374–381.

Paulsen, V.S., Blencke, H.-M., Benincasa, M., Haug, T., Eksteen, J.J., Styrvold, O.B., Scocchi, M., and Stensvåg, K. (2013). Structure-activity relationships of the antimicrobial peptide arasin 1-and mode of action studies of the N-terminal, proline-rich region. PLoS One *8*, e53326.

Podda, E., Benincasa, M., Pacor, S., Micali, F., Mattiuzzo, M., Gennaro, R., and Scocchi, M. (2006). Dual mode of action of Bac7, a proline-rich antibacterial peptide. Biochim. Biophys. Acta *1760*, 1732–1740.

Pounder, R.J., Stanford, M.J., Brooks, P., Richards, S.P., and Dove, A.P. (2008). Metal free thiol-maleimide 'Click' reaction as a mild functionalisation strategy for degradable polymers. Chem. Commun. 5158–5160.

Roy, R.N., Lomakin, I.B., Gagnon, M.G., and Steitz, T.A. (2015). The mechanism of inhibition of protein synthesis by the proline-rich peptide oncocin. Nat. Struct. Mol. Biol. *22*, 466–469.

Rozgonyi, F., Szabo, D., Kocsis, B., Ostorhazi, E., Abbadessa, G., Cassone, M., Wade, J.D., and Otvos, L. (2009). The antibacterial effect of a proline-rich antibacterial peptide A3-APO. Curr. Med. Chem. *16*, 3996–4002.

Saito, G., Swanson, J.A., and Lee, K.-D. (2003). Drug delivery strategy utilizing conjugation via reversible disulfide linkages: role and site of cellular reducing activities. Adv. Drug Deliv. Rev. *55*, 199–215.

Sani, M.-A., Whitwell, T.C., Gehman, J.D., Robins-Browne, R.M., Pantarat, N., Attard, T.J., Reynolds, E.C., O'Brien-Simpson, N.M., and Separovic, F. (2013). Maculatin 1.1 disrupts *Staphylococcus aureus* lipid membranes via a pore mechanism. Antimicrob. Agents Chemother. *57*, 3593–3600.

Seefeldt, A.C., Nguyen, F., Antunes, S., Perebaskine, N., Graf, M., Arenz, S., Inampudi, K.K., Douat, C., Guichard, G., Wilson, D.N., et al. (2015). The proline-rich antimicrobial peptide Onc112 inhibits translation by blocking and destabilizing the initiation complex. Nat. Struct. Mol. Biol. *22*, 470–475.

Separovic, F., Gehrmann, J., Milne, T., Cornell, B.A., Lin, S.Y., and Smith, R. (1994). Sodium ion binding in the gramicidin A channel. Solid-state NMR studies of the tryptophan residues. Biophys. J. *67*, 1495–1500.

Szabo, D., Ostorhazi, E., Binas, A., Rozgonyi, F., Kocsis, B., Cassone, M., Wade, J.D., Nolte, O., and Otvos, L., Jr. (2010). The designer proline-rich antibacterial peptide A3-APO is effective against systemic *Escherichia coli* infections in different mouse models. Int. J. Antimicrob. Agents *35*, 357–361.

Végh, A.G., Nagy, K., Bálint, Z., Kerényi, Á., Rákhely, G., Váró, G., and Szegletes, Z. (2011). Effect of antimicrobial peptide-amide: indolicidin on biological membranes. J. Biomed. Biotechnol. *2011*, 1–6.

Vivcharuk, V., and Kaznessis, Y. (2010). Free energy profile of the interaction between a monomer or a dimer of protegrin-1 in a specific binding orientation and a model lipid bilayer. J. Phys. Chem. B *114*, 2790–2797.

Wu, M., Maier, E., Benz, R., and Hancock, R.E.W. (1999). Mechanism of interaction of different classes of cationic antimicrobial peptides with planar bilayers and with the cytoplasmic membrane of *Escherichia coli*. Biochemistry *38*, 7235–7242.

Zahn, M., Berthold, N., Kieslich, B., Knappe, D., Hoffmann, R., and Sträter, N. (2013). Structural studies on the forward and reverse binding modes of peptides to the chaperone DnaK. J. Mol. Biol. *425*, 2463–2479.

Zasloff, M. (2002). Antimicrobial peptides of multicellular organisms. Nature *415*, 389–395.

Zhou, L., Liu, S.P., Chen, L.Y., Li, J., Ong, L.B., Guo, L., Wohland, T., Tang, C.C., Lakshminarayanan, R., Mavinahalli, J., et al. (2011). The structural parameters for antimicrobial activity, human epithelial cell cytotoxicity and killing mechanism of synthetic monomer and dimer analogues derived from hBD3 C-terminal region. Amino Acids *40*, 123–133.

